Aldosterone mediates activation of the thiazide-sensitive Na-Cl cotransporter through an SGK1 and WNK4 signaling pathway

David J. Rozansky,[1] Tonya Cornwall,[1] Arohan R. Subramanya,[2,3] Shaunessy Rogers,[2] Yong-Feng Yang,[1] Larry L. David,[4] Xiaoman Zhu,[2] Chao-Ling Yang,[2] and David H. Ellison[2,5,6,7]

[1]Department of Pediatrics and [2]Department of Medicine, Oregon Health and Science University, Portland, Oregon, USA. [3]Department of Medicine and Department of Physiology, University of Maryland, Baltimore, Maryland, USA. [4]Department of Biochemistry, [5]Department of Physiology and Pharmacology, and [6]Heart Research Center, Oregon Health and Science University, Portland, Oregon, USA. [7]Portland VA Medical Center, Portland, Oregon, USA.

Aldosterone regulates volume homeostasis and blood pressure by enhancing sodium reabsorption in the kidney's distal nephron (DN). On the apical surface of these renal epithelia, aldosterone increases expression and activity of the thiazide-sensitive Na-Cl cotransporter (NCC) and the epithelial sodium channel (ENaC). While the cellular mechanisms by which aldosterone regulates ENaC have been well characterized, the molecular mechanisms that link aldosterone to NCC-mediated Na^+/Cl^- reabsorption remain elusive. The serine/threonine kinase with-no-lysine 4 (WNK4) has previously been shown to reduce cell surface expression of NCC. Here we measured sodium uptake in a *Xenopus* oocyte expression system and found that serum and glucocorticoid–induced kinase 1 (*SGK1*), an aldosterone-responsive gene expressed in the DN, attenuated the inhibitory effect of WNK4 on NCC activity. In addition, we showed — both in vitro and in a human kidney cell line — that SGK1 bound and phosphorylated WNK4. We found one serine located within an established SGK1 consensus target sequence, and the other within a motif that was, to our knowledge, previously uncharacterized. Mutation of these target serines to aspartate, in order to mimic phosphorylation, attenuated the effect of WNK4 on NCC activity in the *Xenopus* oocyte system. These data thus delineate what we believe to be a novel mechanism for aldosterone activation of NCC through SGK1 signaling of WNK4 kinase.

Introduction

Aldosterone contributes importantly to cardiovascular health and disease. Its physiological roles include modulating arterial pressure and extracellular fluid volume by increasing renal sodium reabsorption. It performs this function by inducing gene transcription in the aldosterone-sensitive distal nephron (ASDN), a tubule segment that extends from the latter portion of the distal convoluted tubule (DCT2) through the medullary collecting duct (1–3). Aldosterone increases the activity of 2 key sodium transporters within this segment: the epithelial sodium channel (ENaC) and the thiazide-sensitive Na-Cl cotransporter (NCC). Aldosterone enhances ENaC-mediated sodium reabsorption primarily by activating transcription of the gene serum and glucocorticoid-induced kinase 1 (*SGK1*), a member of the AGC family of serine/threonine protein kinases that regulates ion transporters (2, 4) and has been genetically associated with predisposing humans to hypertension and the metabolic syndrome (5, 6). SGK1 phosphorylates and suppresses Nedd4-2 ubiquitin ligase activity on ENaC subunits, thereby increasing ENaC surface expression and activity (7). Although aldosterone stimulates NCC activity and increases its abundance, the signal transduction mechanisms responsible for this observation have not been identified (8, 9).

One regulatory system known to affect NCC abundance and activity is the with-no-lysine (WNK) family of serine/threonine kinases (10). Point mutations within the coding region of *WNK4* and mutations to the first intron of the long-sequence WNK1 (*L-WNK1*) gene that result in its overexpression cause familial hyperkalemia and hypertension (FHHt; also referred to as pseudohypoaldosteronism type 2 or Gordon syndrome), a condition of hypertension, hyperkalemia, and hyperchloremic acidosis (11). Investigations with transgenic rodents and heterologous expression systems confirm the importance of WNK4 and WNK1 in regulating NCC (12–16). These experimental results show that WNK4 reduces cell surface NCC expression (17), at least in part, by direct protein-protein interaction, disrupting NCC trafficking to the apical membrane (18, 19). In contrast, L-WNK1 reduces the negative effects of WNK4 on NCC by directly interacting with WNK4 and by indirectly stimulating NCC activity through an enzyme cascade involving oxidative stress-responsive kinase 1 and STE20/SPS1-related proline/alanine-rich kinase (OSR1/SPAK) (20, 21). The effect of L-WNK1 to suppress WNK4-mediated NCC inhibition is dependent on L-WNK1 kinase activity and is blocked by kidney-specific WNK1 (ks-WNK1), a renally expressed, kinase-deficient WNK1 gene product (17, 22). Figure 1A schematically depicts these interactions between kinases and NCC. There have also been reports that WNK4 activates the OSR1/SPAK cascade (23), but the significance of this observation remains unclear, with WNK4 kinase activity shown to be lower than L-WNK1 kinase activity against these targets (24) and also under the influence of angiotensin II (25).

The human *WNK4* gene encodes a protein of 1,243 amino acid residues, containing an N-terminal domain, a kinase domain, 2 coiled-coil domains, and a C-terminal domain (11). In microinjected *Xenopus* oocytes, removal of the 45 C-terminal amino acid region prevents WNK4 inhibition of NCC-mediated sodium transport, implicating this region of the protein, at least in part, as a

Conflict of interest: The authors have declared that no conflict of interest exists.
Citation for this article: *J. Clin. Invest.* **119**:2601–2612 (2009). doi:10.1172/JCI38323.

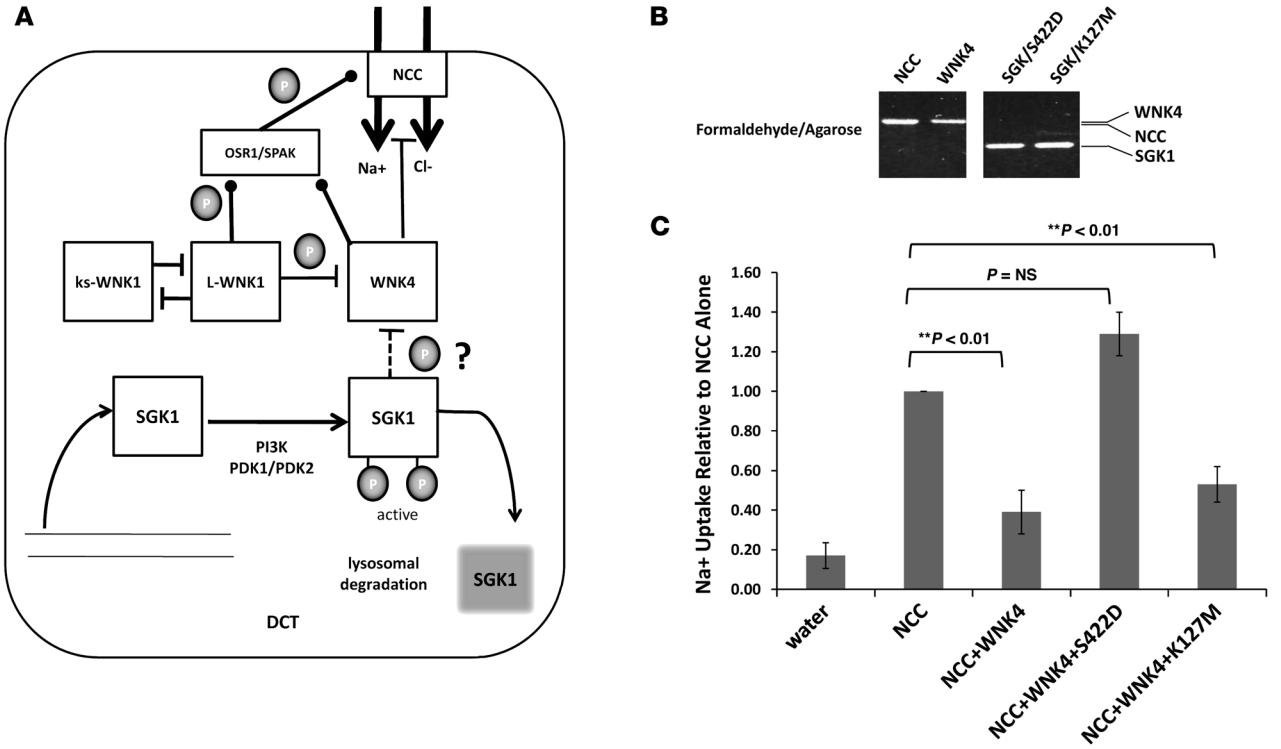

Figure 1

The active form of SGK1 reverses WNK4 inhibition of NCC-mediated Na^+ uptake in *Xenopus* oocytes. (**A**) Schematic diagram of the DCT, outlining the hypothesis of where SGK1 acts to influence WNK4 inhibition of Na^+/Cl^- cotransport (shown by thick arrows). The question mark and dashed line indicate the area of interest for this study. Arrows denote SGK1 movement among inactive, active, and degraded forms. Stimulatory and inhibitory effects are indicated by filled circles and blunt-headed arrows, respectively. Phosphorylation steps are denoted by "P." (**B**) Representative sample of formaldehyde/agarose gel stained with ethidium bromide showing equivalent amounts of SGK/S422D and SGK/K127M cRNA and no obvious degradation prior to injection into oocytes. Lanes were run on the same gel, which was split to maintain the sample order in **C**. (**C**) Relative to NCC alone, WNK4 reduced NCC-mediated Na^+ flux by 60%. The addition of constitutively active SGK1/S422D reversed that effect, whereas addition of kinase-dead SGK1/K127M continued to reduce Na^+ flux. $n = 3$ for each condition (± SEM). Significance (by ANOVA) is indicated.

critical negative regulatory segment (17). While recent work indicates that the N-terminal region may also negatively regulate NCC (26), this C-terminal regulatory domain encompasses amino acids 1198–1243 of human WNK4 and is situated near arginine 1185, an amino acid that causes FHHt in one reported kindred when mutated to cysteine (11).

Multiple proteins have been identified as targets for phosphorylation by SGK1 (27). Many, but not all, are targeted at a serine or threonine within the consensus amino acid sequence R×R××S/T. This sequence motif is also recognized by AKT (also referred to as protein kinase B), and control of the phosphorylation may be influenced by chaperone proteins, such as 14-3-3 (28). S1169 of mouse WNK4 kinase represents one such target for SGK1 phosphorylation, as it is situated within the consensus phosphorylation motif and is highly conserved amongst mammalian species. Note that amino acid residues herein are identified according to the mouse sequence — for example, mouse WNK4 S1169 is homologous to human S1190 — unless indicated otherwise. SGK1 was reported recently to phosphorylate WNK4 at S1169, with functional effects on ENaC and renal outer medullary K^+ channel (ROMK) (29).

In this study, we tested the hypothesis that aldosterone regulates NCC activity through interactions between SGK1 and WNK4 kinase. Our results indicate that SGK1 reverses WNK4 inhibition of NCC activity. SGK1 bound and phosphorylated WNK4, but the predominant site of phosphorylation was a site within the C-terminal negative regulatory domain of WNK4 that was not to our knowledge described previously. We further clarified that this site of SGK1 phosphorylation was 1 of 2 sites necessary for relieving the inhibition of WNK4 on NCC electroneutral cotransport, thereby providing what we believe to be the first information about the signal transduction pathway that links aldosterone and NCC in the kidney.

Results

SGK1 attenuates the effects of WNK4 on NCC. SGK1 may modulate WNK4 regulation of NCC, integrating with the putative signals from L-WNK1, ks-WNK1, and OSR1/SPAK (Figure 1A). To study the influence of SGK1 and WNK4 directly on NCC function, we measured $^{22}Na^+$ uptake by *Xenopus laevis* oocytes injected with cRNA to express these proteins. After confirming previous results indicating that SGK1 does not affect $^{22}Na^+$ uptake by NCC directly (13) and that the cRNA had not been degraded (Figure 1B), we tested how SGK1 alters WNK4 inhibition of NCC-mediated Na^+ transport. When WNK4 was expressed with constitutively active SGK1 (SGK1/S422D), WNK4 inhibition of NCC was reversed and there was no difference in $^{22}Na^+$ uptake compared with NCC alone

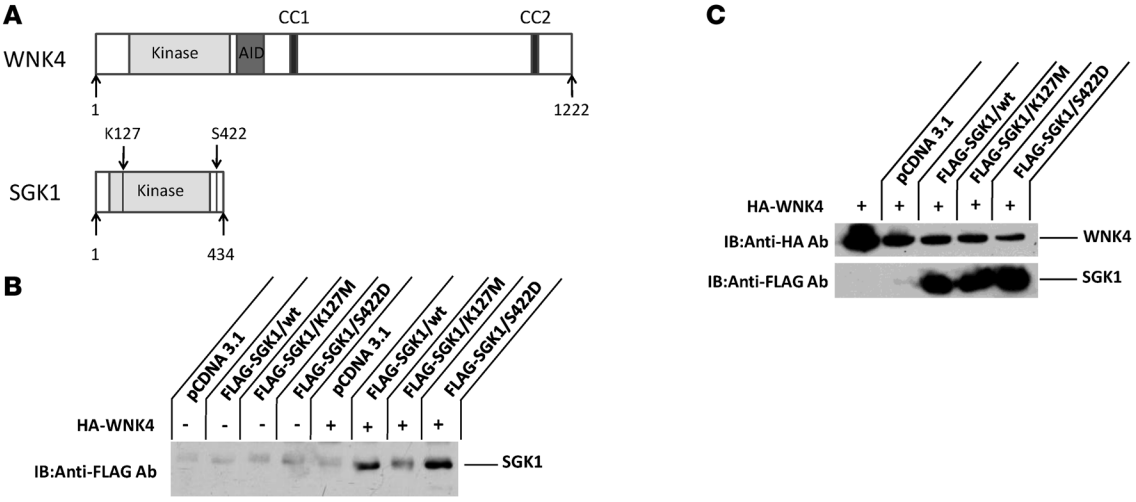

Figure 2

SGK1 associates with WNK4. (**A**) Schematic of WNK4, showing kinase domain, autoinhibitory domain (AID), and coiled-coil domains (CC), and of SGK1, showing kinase domain and K127M (kinase-dead) and S422D (constitutively active) mutation locations. (**B**) HEK293 cells were transfected with FLAG-tagged SGK1 isoforms or vector pCDNA3.1 in the presence or absence of full-length HA-tagged WNK4. After lysis and isolation with anti-HA sepharose beads, coimmunoprecipitation between SGK1 and WNK4 was tested by immunoblot using anti-FLAG antibody. The blot revealed the presence of SGK1 protein bound to WNK4. WNK4 associated with SGK1 with greater signal for wild-type and S422D isoforms than for the K127M isoform. The background band evident in all lanes is the IgG light chain, which migrated on the gel at a slightly larger molecular weight than SGK1. (**C**) Immunoblots from transfected cell lysates only, confirming the presence of WNK4 and SGK1 for interactions tested in **B**. Blots in **B** and **C** are representative samples from 2 experiments.

(Figure 1C). In contrast, kinase-dead SGK1/K127M did not block the effect of WNK4. Microinjection into the oocytes of 12.5 ng SGK1 isoform, 10 ng NCC, and 5 ng WNK4 cRNA yielded the results shown in Figure 1B. In a separate study, microinjecting 2 ng of either SGK1/S422D or SGK1/K127M cRNA into this system did not alter the inhibitory effect of WNK4 on NCC (data not shown), which suggests that SGK1 acts in a dose-dependent manner. Taken together, these results suggest that a phosphorylation event is essential for the observed effect of SGK1 on WNK4, or that SGK1/S422D interacts sterically with WNK4 to a greater degree than does SGK1/K127M to disrupt WNK4 action on NCC.

Coimmunoprecipitation of SGK1 and WNK4. To determine whether SGK1 and WNK4 kinases (Figure 2A) form a protein complex in mammalian cells, we performed immunoprecipitation analysis. HEK293 cells were transfected with HA-tagged WNK4 and FLAG-tagged SGK1 (including wild-type, S422D, and K127M). Harvested cell lysates were precipitated with monoclonal anti-HA sepharose beads and eluted with SDS sample buffer before immunoblot detection. SGK1 associated with WNK4 in a protein complex in mammalian kidney cells, and more SGK1 was precipitated with the constitutively active form than with the kinase-dead form (Figure 2B). Cells transfected with SGK1 in the absence of HA-WNK4 yielded no evidence of a coimmunoprecipitation product. Immunoblot of the cell lysates showed equivalent amounts of protein product in all transfections (Figure 2C).

SGK1 phosphorylates WNK4. We next tested whether SGK1 is capable of phosphorylating WNK4. Our results indicated that HA-WNK4 was phosphorylated by SGK1 when precipitated from transfected mammalian embryonic kidney cells (Figure 3A). Bacterially derived glutathione-S-transferase (GST) and the GST–Nedd4-2 — a well-documented target of SGK1 — served as negative and positive controls, respectively.

Although these data suggest that SGK1 phosphorylates WNK4, WNK kinases are capable of autophosphorylation and cross-phosphorylation (30). Deleting SGK1 from the incubation mixture reduced, but did not eliminate, WNK4 phosphorylation (Figure 3B). This finding raised the possibility that the observed phosphorylation resulted from WNK4 autophosphorylation. To eliminate this confounder, we next tested whether an autophosphorylation-deficient WNK4 was phosphorylated by SGK1. In order to be activated, WNK kinases must be autophosphorylated at a serine in the activation loop (31–33). HA-WNK4/S332A, which is mutated on the essential serine and thus autophosphorylation deficient, was still phosphorylated in the absence of SGK1 (Figure 3B). However, SGK1 further enhanced phosphorylation, which suggests not only that SGK1 phosphorylates WNK4, but also that one or more other kinases are present in the reaction mixture. Recently, Yu and colleagues reported that the carboxyl terminus of WNK4 associates with a novel kinase in pulldown assays (34); the present data are entirely consistent with this prior observation.

C-terminal WNK4 as a target for SGK1 phosphorylation. To confirm that SGK1 phosphorylates WNK4, we used bacterially derived GST-WNK4 fusion proteins, which should not be associated with other mammalian kinases, in an SGK1 kinase assay. We focused our efforts on the C-terminal region of mouse WNK4, where a canonical SGK1 phosphorylation target sequence lies (S1169, analogous to human WNK4 S1190; ref. 27). This serine is close to an FHHt mutation site that was previously shown by Lifton and colleagues to be phosphorylated by SGK1 (11, 29).

GST-WNK4/1112–1222, a fusion protein containing a fragment of WNK4 that includes both the C-terminal NCC-regulatory region and the identified SGK1 phosphorylation site 1169, was compared in an SGK1 kinase assay with fusion proteins in which the index serine was mutated to alanine (S1169A) or the SGK1

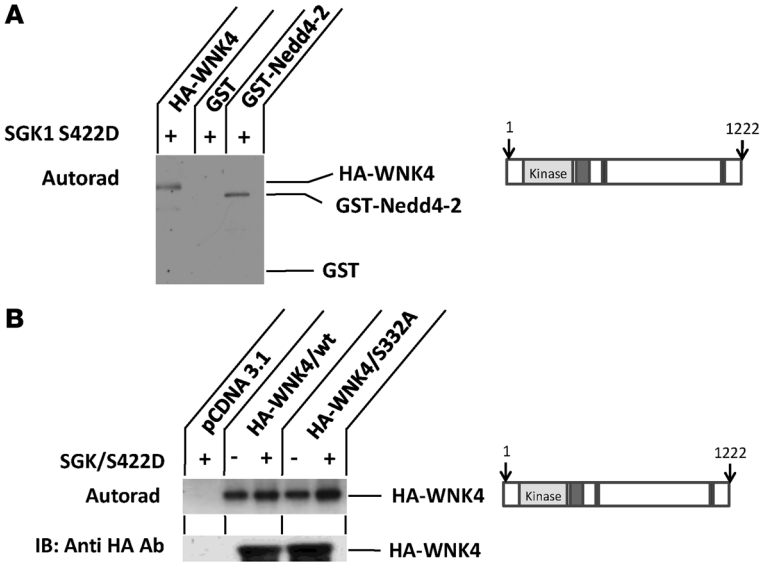

Figure 3

SGK1 kinase activity on full-length WNK4. (**A**) SGK1 kinase assay testing HA-tagged WNK4, GST-Nedd4-2, and GST alone as substrates. WNK4 and GST-Nedd4-2, but not GST alone, were phosphorylated. (**B**) SGK1 kinase assay of HA-tagged WNK4 and autophosphorylation-deficient WNK4 (S332A). A stronger signal was noted in the presence of SGK1, but its absence did not eliminate the signal. The immunoblot below confirmed equivalent amounts of the 2 WNK4 isoforms used in the SGK1 kinase assay above. Blots are representative samples from 2 experiments.

recognition sequence was altered to the identified FHHt mutation (R1164C). The S1169A mutation reduced phosphorylation only modestly, while R1164C had no effect (Figure 4A).

Because the S1169A mutation did not eliminate phosphorylation of GST-WNK4/1112–1222 by SGK1, we altered our strategy to identify sites at which SGK1 phosphorylates WNK4. We separated the fusion protein into 2 pieces — fragment 1178–1222, consisting of the 45–amino acid C-terminal domain, and fragment 1112–1177, containing the remainder — and then subjected them to an in vitro SGK1 kinase assay. Robust phosphorylation of WNK4/1112–1222 was maintained in the C-terminal, WNK4/1178–1222 fragment, with an intense autoradiographic signal (Figure 4B). In contrast, the fragment containing S1169, WNK4/1112–1177, had a much lower intensity, comparable to the WNK4/1127–1179 fragment, previously shown to be an SGK1 substrate by Ring et al. (29). GST alone served as a negative control, with no phosphorylation noted on exposure to SGK1; Coomassie Blue staining confirmed that equivalent protein quantities were loaded onto each lane. In addition, S1169 was confirmed as the site of SGK1 phosphorylation within the WNK4/1112–1177 fragment, because mutation of this fragment to S1169A eliminated detectable autoradiographic signal (Figure 4C).

We postulated that the observed greater than 10-fold autoradiographic signal in GST-WNK4/1178–1222 compared with GST-WNK4/1112–1177 resulted from the presence of multiple SGK1 phosphorylation sites in this region; 10 of the 45 amino acids in this short protein fragment were either serines or threonines (Figure 5A). In order to identify residues within this fragment that are phosphorylated by SGK1, we used liquid chromatography/mass spectrometry/mass spectrometry (LC/MS/MS). An SGK1 kinase assay using cold ATP was performed on GST-WNK4/1178-1222, and the product was trypsinized and subjected to LC/MS/MS analysis. This analysis identified 80% of the sequence of the GST-WNK4 construct, as well as 39 of 45 residues of the C-terminal region of the WNK4. The only phosphorylation site identified in the recovered sequence was in peptide 246–260 of the construct, and the modification site was localized to S248. Both *y* and b ion fragment series localizing the +80 mass shift to S248 were assigned in the MS/MS spectra, as well as the characteristic neutral loss of 98 mass units from the doubly charged parent ion as a result of loss of phosphate from the peptide (Figure 5B). S248 of the fusion protein corresponded to S1196 of mouse WNK4.

Site-directed mutagenesis of S1196 to alanine resulted in a GST-WNK4 fusion protein that underwent an in vitro SGK1 kinase assay using ^{32}P-γ-ATP. As shown in Figure 5C, the autoradiographic signal was completely eliminated by this single mutation, which suggests that S1196 is the predominant phosphorylation site for SGK1 in the C-terminal region of WNK4.

We next tested whether SGK1 also targeted mouse WNK4/S1196 for phosphorylation in mammalian cell lysates. HEK293 cells were transfected with 1 of 4 HA-tagged WNK4/1112–1222 plasmid constructs (wild type, S1169A, S1196A, and S1169A/S1196A), and fusion proteins were immunoprecipitated with anti-HA sepharose beads, washed, and subjected to the SGK1 kinase assay. The anti-WNK4 immunoblot (Figure 6A) showed equivalent levels of WNK4 C-terminal fragment protein among all 4 lysates. We applied these isolates to the in vitro SGK1 kinase assay; each was exposed to ^{32}P-γ-ATP in the presence or absence of SGK1. In the absence of SGK1, no apparent phosphorylation was recorded for any isolate. In the presence of SGK1, there was phosphorylation in each lane, including the double mutant; the intensity of the signal, however, varied by mutant, with wild-type appearing to be the most intense and the double mutant the least so (Figure 6A).

We used densitometry to quantify the differences in phosphorylation by normalizing the autoradiographic signal to the protein signal in Figure 6A for each WNK4 fragment. There was a loss of signal for both of the single serine mutants and the double mutant, with the latter having the weakest signal (Figure 6B). In addition, the reduction in signal for the double mutant was nearly additive: relative to wild type, HA-WNK4/1112–1222,S1169A reduced the signal modestly, HA-WNK4/1112–1222,S1196A decreased it by 28%, and when both mutations were present, the signal was diminished by an average of 57%. This supports S1169 and S1196 as targets of SGK1 phosphorylation within mammalian cells. The persistence of a signal in the double mutant illustrates the potential complexity of SGK1's activity within the C-terminal region of WNK4. In the context of mammalian cells, SGK1 may target another serine or threonine in this region as a result of a posttranslational modification not present in bacterially derived WNK4; alternatively, another kinase that targets this region, such as the one characterized by Yu et al. (34), may be SGK1 dependent and have coimmunoprecipitated with the HA-tagged WNK4 fragments.

WNK1 and SGK1 phosphorylate WNK4 at the same site. The current data indicate that SGK1 associates with WNK4 and inhibits its

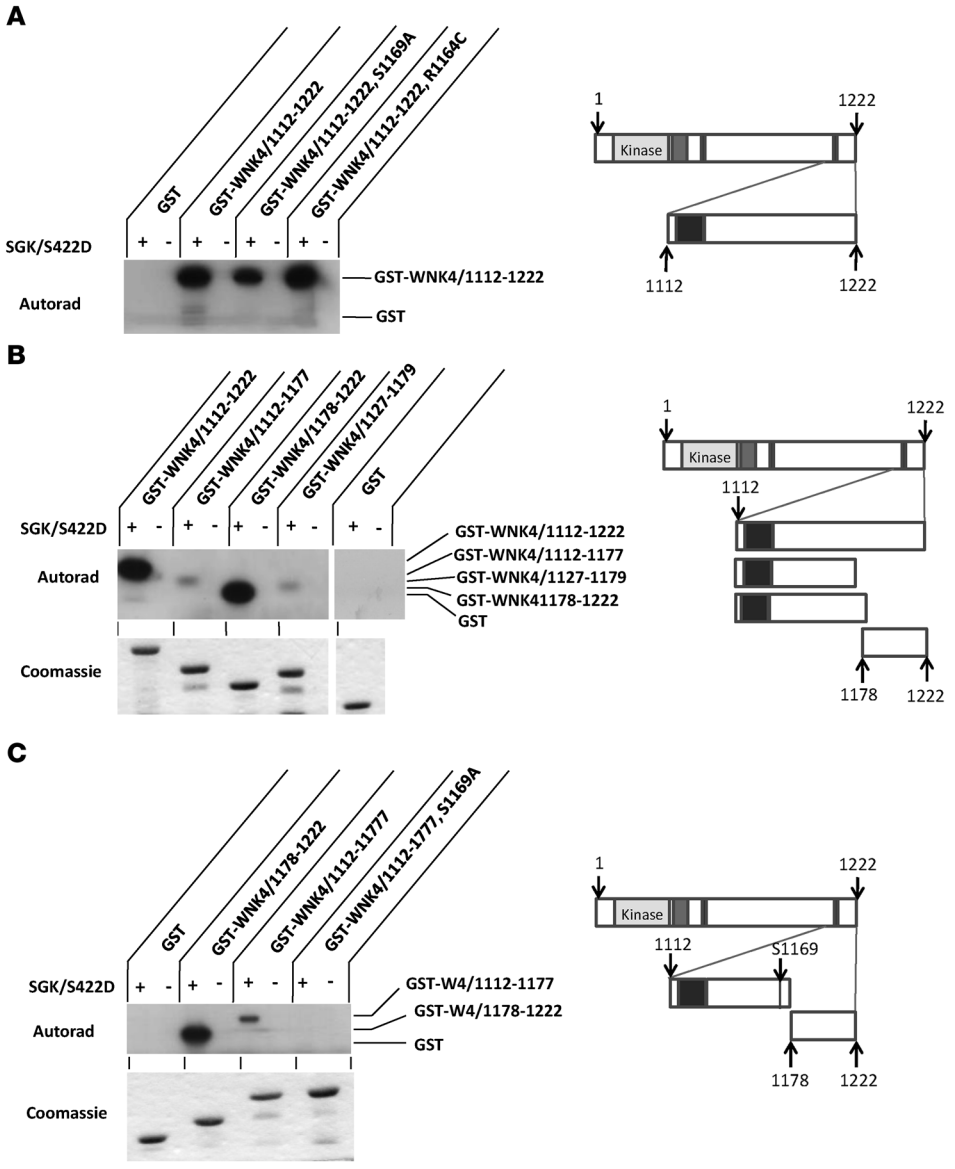

Figure 4
SGK1 phosphorylates more than 1 serine/threonine site of the C-terminal region of WNK4. GST-WNK4 fusion proteins from 1112 to 1222 were isolated from bacteria and subjected to an SGK1 kinase assay. Shown with each panel is a schematic of the WNK4 region of interest and the approximate size of the GST-fusion protein. (**A**) SGK1 kinase assay of 0.8 μg GST-WNK/1112–1222 and isoforms conforming to mutants associated with FHHt (R1164C) and putative SGK1 phosphorylation target (S1169A). Autoradiographic signal was equivalent for wild-type and R1164C, with a slight reduction in signal for S1169A. (**B**) C-terminal GST-WNK4 deletion constructs showed much stronger signal for 1178–1222 compared with 1112–1177 or 1127–1179. Below, Coomassie Blue staining of protein preparations confirmed that equivalent amounts of the 5 substrates were used in the study above. Data are from 2 gels run simultaneously. (**C**) S1169 was confirmed as the only target of SGK1 phosphorylation in WNK4 fragment 1112–1177. Shown below is Coomassie Blue staining of 4 protein preparations. Blots in **A**–**C** are representative samples from 3 experiments.

action on NCC, and furthermore that SGK1 phosphorylates the carboxyl terminus of WNK4 at S1196. We have shown previously that L-WNK1 associates with WNK4 and inhibits its action on NCC (13); we also showed that L-WNK1 phosphorylates the carboxyl terminus of WNK4 (15), but those results did not identify specific serine or threonines involved. Here, we tested whether WNK1 and SGK1 share phosphorylation motifs within the carboxyl terminus of WNK4. By an in vitro L-WNK1/1–491 kinase assay with GST-WNK4/1172–1222 as the substrate, we observed that L-WNK1 strongly phosphorylated this WNK4 fragment (Figure 6C). Moreover, mutating S1196 to alanine substantially reduced, but did not abolish, phosphorylation, and mutating 2 other serines in the WNK4 carboxyl terminus did not affect the level of phosphorylation.

C-terminal phosphorylation of WNK4 reverses WNK4 inhibition of NCC activity. With SGK1 and WNK1 kinase targeting serines that lie near or within the C-terminal negative regulatory region of WNK4 (17), we tested how phosphorylation of these sites might alter WNK4 regulation of NCC-mediated Na^+/Cl^- cotransport. S1169 and S1196 of WNK4 were mutated into aspartate to mimic phosphorylation of final WNK4 protein products. cRNA for wild-type C-terminal WNK4, single mutants WNK4/S1169D and WNK4/S1196D, and the double mutant WNK4/S1169D,S1196D were microinjected with NCC into *Xenopus* oocytes, confirmed for lack of degradation (Figure 7A), and compared for $^{22}Na^+$ uptake with oocytes injected with NCC alone (Figure 7B). This experiment revealed that whereas the single mutations WNK4/S1169D and WNK4/S1196D reduced NCC function to levels comparable to that of WNK4 alone, the double mutation did not reduce Na^+ transport significantly compared with NCC alone. The finding suggested that targeted phosphorylation of WNK4 at these 2 serines in the carboxyl terminus of WNK4 was sufficient to prevent WNK4 kinase inhibition of NCC activity.

Discussion

Arterial pressure is regulated chronically by renal NaCl excretion. The renin/angiotensin/aldosterone (RAAS) system plays a dominant role in controlling renal NaCl excretion; drugs that interfere

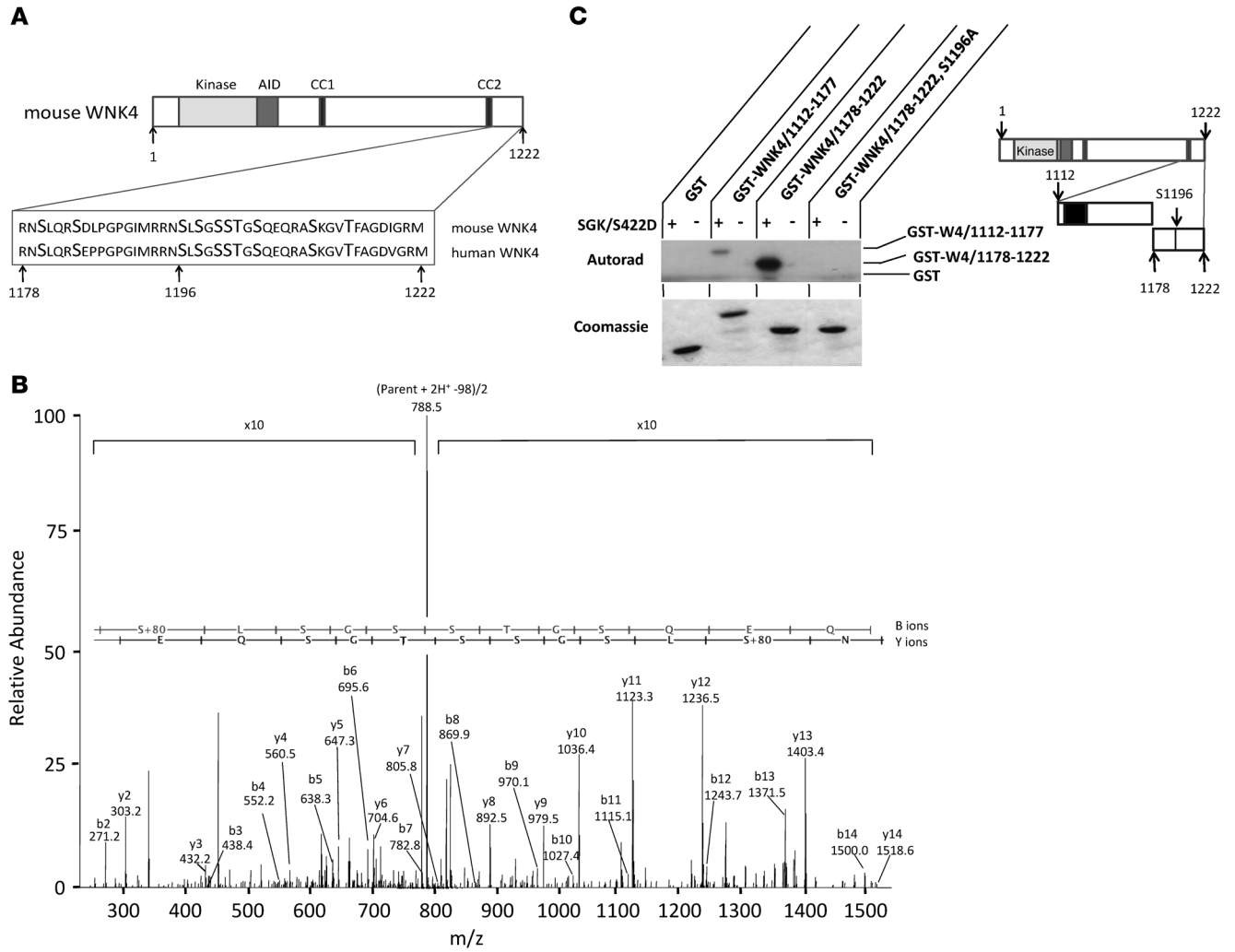

Figure 5

Within the 45–amino acid C-terminal NCC negative regulatory region of WNK4/1178–1222, S1196 acts as a single target of SGK1 phosphorylation. (**A**) Amino acid sequence of this WNK4 region contains 10 serines and threonines. (**B**) MS/MS spectrum of peptide 246–260 from a tryptic digest of GST-WNK4/1178–1222, localizing phosphorylation to residue S248 in the construct (corresponding to residue S1196 of mouse WNK4) after incubation with SGK1 kinase. An uninterrupted y and b ion series was observed in the fragment ion spectra, as well as a characteristic major doubly charged neutral loss ion at *m/z* 788.5 resulting from the loss of phosphate. Because of the intensity of this neutral loss ion, the intensities of the other areas of the spectrum increased 10-fold. The inset sequence of the peptide is aligned with the corresponding fragment ions of the y and b ion series. (**C**) In vitro SGK1 kinase assay confirmed that S1196 was the only SGK1 phosphorylation site in the region 1178–1222 from bacterially derived fusion fragments. The single mutation of WNK4/1178–1222 S1196A was not phosphorylated by SGK1, whereas wild-type and fragment 1112–1177 yielded robust and weak signals, respectively. Shown below is Coomassie Blue staining of the 4 protein preparations used for the SGK kinase assay. *n* = 3. The schematic diagram denotes the C-terminal WNK4 region and the approximate size of the GST-fusion proteins.

with this system are among the most commonly prescribed agents in clinical medicine. The RAAS system reduces urinary NaCl excretion in part by stimulating NCC activity along the distal nephron. Aldosterone is an important mediator of this effect, increasing NCC activity, abundance, and phosphorylation (8, 9, 35, 36). Histological studies on human and mammalian kidney tissue demonstrate that DCT cells express all of the molecular components required for mineralocorticoid activity and are influenced dynamically by exposure to aldosterone (37, 38). Yet the signal transduction mechanisms that link aldosterone and NCC have remained obscure.

One signal transduction pathway that to our knowledge had not previously been explored involves WNK kinases. WNK4 kinase reduces NCC surface expression when tested using heterologous expression systems and mammalian kidney tubular cells (12, 13, 17, 39). WNK4 also inhibits NCC activity and abundance in situ; mice with extra copies of the wild-type *WNK4* gene exhibit DCT segments that are hypoplastic, with diminished NCC expression and activity (38). Here, we report that the aldosterone-induced protein SGK1 stimulated NCC activity through a WNK4-dependent mechanism. Our findings support a mechanism whereby SGK1 targets 2 serines for phosphorylation near the carboxyl terminus of WNK4, attenuating WNK4 inhibition of NCC activity. Although the precise details of the interaction between SGK1 and WNK4 kinase will require fur-

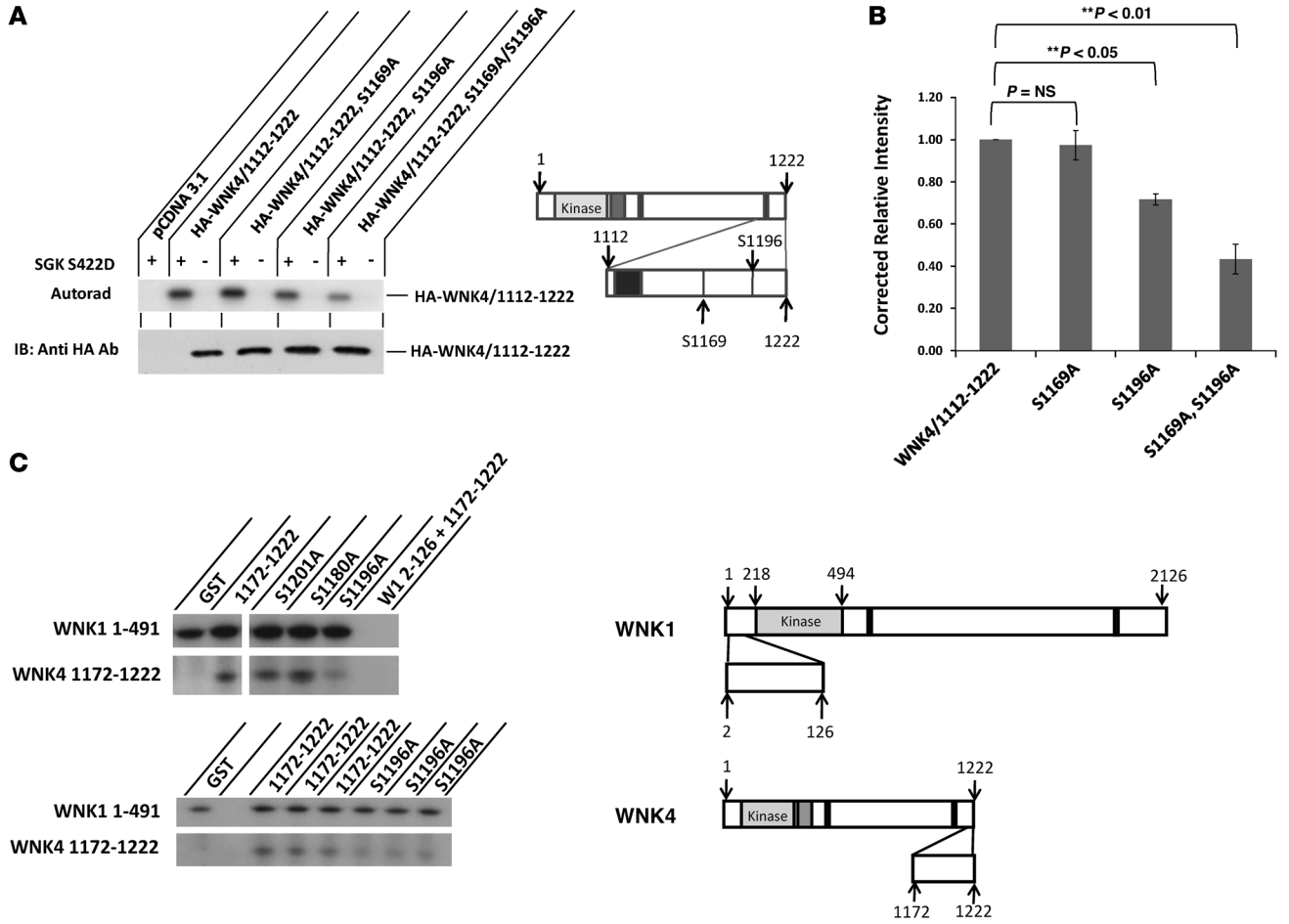

Figure 6

SGK1 and WNK1 phosphorylate S1196 of the C-terminal fragment of WNK4 kinase. (**A**) HA-tagged WNK4/1112–1222 was mutated at S1169 and/or S1196 and isolated by immunoprecipitation from HEK293 cells. In vitro SGK1 kinase assay of these fragment isoforms showed that wild-type and S1169A had higher levels of autoradiographic signal compared with S1196A or the double mutant S1169A/S1196A. Immunoblot shown below demonstrates comparable protein levels of the 4 fragments used above. $n = 3$. (**B**) Average ratios of autoradiographic densitometric signal to immunoblot signal for each fragment, which revealed additive properties with reduction in signal as index serines were removed. While S1169A trended lower, significance in signal reduction was noted for S1196A and the double mutant. Significance (by ANOVA) is shown. $n = 3$ for each condition (± SEM). (**C**) Schematic diagram shows the constructs used in a WNK1 kinase assay for both WNK1 and WNK4. The top blot shows WNK1 kinase assays of GST-WNK1 fusion enzymes in the presence of substrates: GST alone, or GST-WNK4 C-terminal fragment 1172–1222 and specific serine-to-alanine mutations. The first row demonstrated that GST-WNK1/1–491 had autophosphorylation properties, whereas GST-WNK1/2–126 did not. The second row indicated that C-terminal serine-to-alanine mutations of WNK4 reduced the phosphorylation signal for WNK4/S1196 exclusively. In the bottom blot, the first row replicates indicated equal autophosphorylation of WNK1. In the second row, the WNK4/S1196A substrates had a weaker signal than that of their wild-type counterparts.

ther elucidation, this observation provides what we believe to be the first molecular insight into the signal transduction pathway mediating aldosterone effects on NCC: aldosterone acts in the distal nephron DCT2 segment, where both NCC and ENaC are expressed, and it acts primarily by altering gene transcription, including enhancing SGK1 mRNA and its subsequent protein product. SGK1 then binds to and phosphorylates WNK4, thereby reversing the inhibitory effect of WNK4 on NCC. The net effect of aldosterone, then, was to increase NaCl reabsorption within the distal convoluted tubule.

Previously, we reported that SGK1 does not affect NCC activity when assessed using heterologous expression systems (13), but those experiments were conducted in the absence of WNK kinases. Although the current studies also used heterologous expression systems, the physiological relevance of our results is consistent with recent work in SGK1 knockout mice. Fejes-Toth and colleagues reported that when subjected to dietary NaCl restriction, $SGK1^{-/-}$ mice exhibit a phenotype of sodium wasting with reduced NCC abundance compared with wild-type animals (40). Their results confirm that in vivo, in the absence of SGK1, stimulating the RAAS system results in reduced expression of NCC compared with control animals. These studies therefore corroborate that NCC regulation by the RAAS can be dependent on the presence of SGK1 activity. The *extent* of that dependence, however, should be considered only partial, because mineralocorticoids likely have multiple mechanisms to activate renal sodium transport, as has been shown in the SGK1 knockout mouse (41); moreover, angiotensin II may also play a role in regulating SGK1 (42).

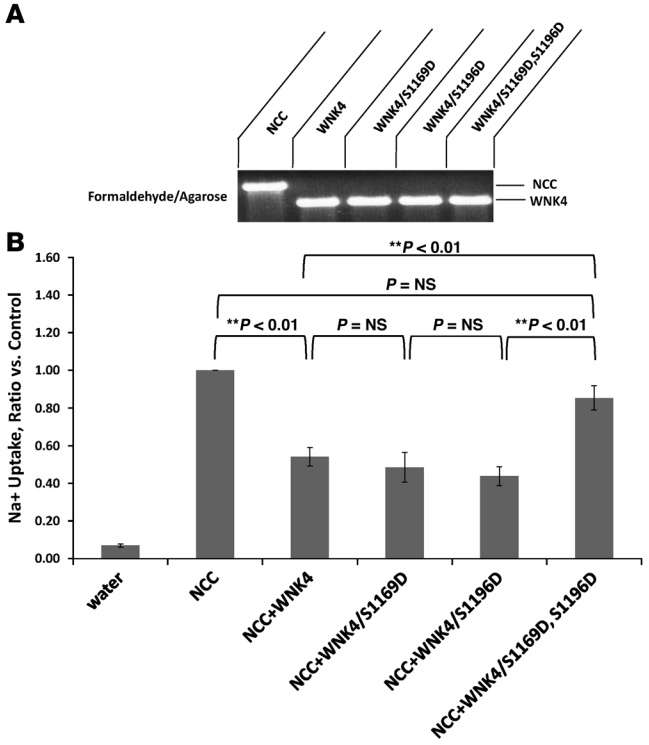

Figure 7
The double aspartate WNK4 mutant S1169D,S1196D fails to inhibit NCC activity in *Xenopus* oocytes. (**A**) Formaldehyde/agarose gel stained with ethidium bromide showed equivalent amounts of cRNA and no obvious degradation for each WNK4 construct prior to oocyte injections. (**B**) Relative to NCC alone, WNK4 reduced NCC-mediated Na^+ flux by 50%. Single aspartate mutations at either S1169 or S1196 did not significantly impair the ability of WNK4 to block NCC activity. However, WNK4 containing both serine-to-aspartate mutations was unable to reduce Na^+ uptake. $n = 3$ for each condition (± SEM). Significance (by ANOVA) is shown.

The present results also indicate that the kinase activity of SGK1 on WNK4 is required for it to affect NCC function. The results in Figure 1 show that kinase-dead SGK1 did not affect Na^+ uptake, while the constitutively active form of SGK1 did. Ring et al. reported that SGK1 phosphorylates WNK4 on S1169, thereby relieving the ENaC-inhibiting effects of WNK4 (29). Mutating this serine to alanine abrogated the effect of SGK1 on ENaC, but the same mutation reportedly had no effect on NCC. This observation suggests that phosphorylation of S1169 on WNK4 is not sufficient to relieve NCC inhibition.

In order to identify WNK4 phosphorylation sites responsible for the effect on NCC, we focused on the carboxyl terminus of the protein. Because deletion of a C-terminal 45 amino acid fragment reversed WNK4's negative regulatory effect on NCC activity (17), we used an unbiased approach to detect phosphorylation sites within this region and detected 2 sites at which SGK1 phosphorylated WNK4. S1169 is within the canonical SGK1 phosphorylation sequence of R×R××S/T and is identical to the serine previously shown by Ring, Lifton, and colleagues to be phosphorylated by SGK1 (29). To our knowledge, S1196 has not previously been described as an SGK1 phosphorylation site, but it does possess an arginine in a –3 position (like a canonical SGK1 target sequence) and an isoleucine at the –5 position. This sequence motif was not tested by Cohen et al. in their reports on SGK1/AKT targeting (27, 43), but others have reported that SGK1 may phosphorylate at serine or threonine residues unrelated to the canonical sequence (43, 44). Comparison of the strength of phosphorylation at the 2 sites showed that phosphorylation was 3- and 10-fold more intense at the S1196 site than at the S1169 site when the WNK4 fragment was isolated from mammalian and bacterial cells, respectively. Of note, S1196 was not included in the WNK4 fragment tested by Ring et al. (29).

It is striking that the effect of SGK1 on WNK4 and NCC is similar to the effect of L-WNK1 on WNK4 and NCC. The results of kinase assays indicated that L-WNK1 and SGK1 share phosphorylation targets and share similar effects on WNK4. Our results conflate 2 regulatory pathways within the mammalian distal nephron, the aldosterone-SGK1 pathway and the WNK kinase pathway. This observation is not surprising, as FHHt, the genetic disease caused by mutations in WNK kinases, is one in which several consequences of aldosterone action are dissociated. The dissociation, or aldosterone paradox, is based on 2 distinct observations: (a) with volume depletion, activation of the RAAS system restores the body's volume without affecting plasma potassium levels; and (b) when hyperkalemic, the kidney induces kaliuresis, restoring potassium levels without altering body volume.

WNK4, WNK1, and SGK1, and their interactions in the distal nephron, have been proposed by several investigators to be the fulcrums that explain this differential response to aldosterone (19, 29, 37, 45, 46). Figure 8 schematically depicts how SGK1's action on WNK4 within the DCT2 and the collecting duct may add to our understanding of the aldosterone paradox. SGK1, WNK1, and WNK4 interact to regulate electroneutral and electrogenic transport along the distal nephron. According to this model, conditions in which aldosterone secretion is stimulated by angiotensin II (e.g., extracellular fluid volume depletion) would enhance SGK1 activity, inactivating the negative regulatory effects of WNK4 along with L-WNK1 and thereby stimulating NCC, ENaC, and ROMK and leading to balanced absorption of Na^+ with Cl^- as well as Na^+ in exchange for K^+. In contrast, conditions in which aldosterone secretion is stimulated by hyperkalemia would increase the ks-WNK1/L-WNK1 ratio, thereby inhibiting L-WNK1 and allowing WNK4 to suppress NCC activity. This would shift the predominant effect of aldosterone to Na^+/K^+ exchange in the collecting duct and away from NCC activation in the DCT, where ENaC and ROMK would be stabilized by SGK1 and other aldosterone-initiated mechanisms (47–49). We surmise that processes that promote inactivation of WNK4 hold the key to unraveling the paradox and that these processes are dependent on elements activated by the RAAS that are not caused by aldosterone alone. SGK1, with its activity dependent on PI3K and its expression regulated by both transcription and intracellular degradation pathways (50–52), could be one target of an elevated RAAS. Although it should be emphasized that this hypothesis remains conjectural, the current results indicate that WNK kinases and SGK1 are best viewed as distinct components of a comprehensive signal transduction pathway in the distal nephron, one that determines the balance between NaCl absorption and Na^+/K^+ exchange. In addition, as the precise details of how WNK4 integrates physiologically with the OSR1/SPAK cascade onto NCC are worked out (23, 25, 38), the present study supports that the net effect of SGK1 is to increase NaCl absorption by NCC through a relationship with WNK4.

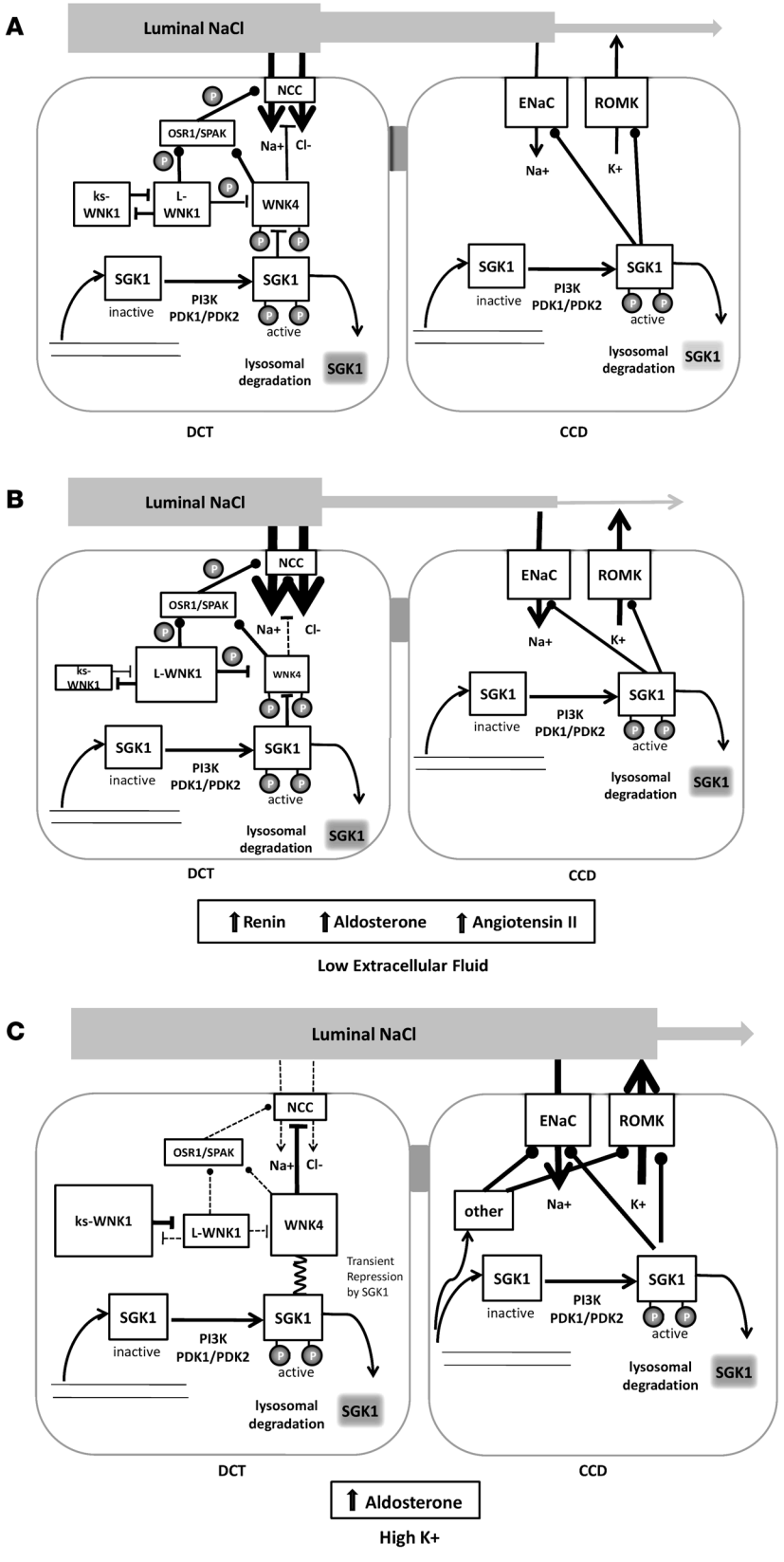

Figure 8

WNK4, WNK1, SGK1, and aldosterone paradox hypothesis. WNK4 kinase inhibits NCC activity. Multiple secondary messengers modulate WNK4 action. L-WNK1 inhibits WNK4, but is suppressed by ks-WNK1. L-WNK1 also phosphorylates OSR1/SPAK, thereby activating NCC. Symbols are as in Figure 1; secondary messenger proteins and ion transporter sizes vary relative to their proposed activity. (**A**) Our results suggest that SGK1, induced transcriptionally by aldosterone and activated by PI3K, negatively regulates WNK4's action on NCC by phosphorylating 2 C-terminal serines of WNK4. SGK1 also positively effects ENaC and ROMK activity in the cortical collecting duct (CCD) through regulatory pathways that include SGK1. (**B**) Schematic proposal of renal response to hypovolemia, through hyperreninemia and/or stimulation of angiotensin II and aldosterone. Here SGK1 and WNK1 target similar C-terminal WNK4 serines for phosphorylation, relieving the WNK4 inhibitory effect on NCC, increasing NCC-mediated Na^+/Cl^- cotransport (shown by arrow thickness) while diminishing the regulatory value of SGK1 and other mechanisms in the CCD that lead to K^+ secretion. (**C**) Schematic proposal of renal response to aldosterone stimulation by hyperkalemia. In the DCT there is upregulation of ks-WNK1 activity, which — by squelching L-WNK1 — leads to heightened WNK4 activity, low SPAK/OSR1 activity, and reduced NCC-mediated NaCl transport. We surmise that SGK1 has a transient effect on WNK4 with downstream ENaC and ROMK activation by SGK1 and other aldosterone-sensitive mechanisms, restoring potassium balance without affecting extracellular volume.

Methods

Xenopus oocyte studies

All animal experiments described herein received approval from the Oregon Health and Science University Institutional Animal Care and Use Committee. Experiments using radioisotopes were approved and monitored by the Oregon Health and Science University Environmental Health and Radiation Safety office. Oocytes surgically collected from *X. laevis* frogs were microinjected with in vitro transcribed cRNA of NCC, WNK4, and SGK1. The injected oocytes were immersed in medium containing $^{22}Na^+$. Functional activity of expressed NCC in the presence of WNK4 and SGK was gauged by $^{22}Na^+$ uptake, as measured by liquid scintillation.

To prepare the cRNA, wild-type and specific mutations of mouse NCC, WNK4, and SGK1 were subcloned into the *Xenopus* expression vector pGH19 by standard methods. The WNK4 construct was prepared by PCR using the full-length WNK4/pGH19 as a template and forward primers containing restriction enzyme sites just 5′ to the nucleotide sequences corresponding to amino acids 167 and 445. We used these N-terminal deletions of WNK4 because their respective effects on NCC-mediated sodium transport have been shown to be reproducible (13, 17, 30, 39) and specific for the C-terminal negative regulatory domain (17). The constitutively active SGK1/S422D and kinase-dead SGK1/K127M mutations were prepared using the Quik Change Site-Directed Mutagenesis kit (Stratagene). All constructs were confirmed by sequencing.

Injection of cRNA and measurement of sodium transport were performed as previously reported (13). In brief, linearized plasmid vectors were used as template in a mMESSAGE mMACHINE kit (Ambion) to generate cRNA. On day 1, *Xenopus* oocytes were digested with collagenase after surgical collection and sorted within 24 hours. On day 2, the animal poles of mature oocytes were injected with 5–10 ng of each cRNA in 50 nl water per single oocyte. For each treatment group, 30–40 oocytes were injected in a single day, and the injections were repeated on 3 separate days. These oocytes were incubated at 18°C overnight in fresh ND96 solution. On day 3, the ND96 was replaced with fresh ND96. On day 4, oocytes were washed 3 times in Cl^--free ND96. On day 5, intact oocytes were washed 3 times in Cl^-/K^+-free ND96 and incubated at room temperature. This medium was then replaced with medium containing $^{22}Na^+$, and the oocytes were incubated in the presence of $^{22}Na^+$ for 1 hour at 30°C. Oocytes were washed 4 times at the end of the $^{22}Na^+$ incubation, transferred to scintillation vials, and lysed by the addition of 10% SDS. After scintillation fluid was added, intracellular $^{22}Na^+$ (representing Na^+ uptake) was measured.

Immunoprecipitation and SGK1 kinase assays

Epitope-tagged WNK4 and SGK1 plasmid constructs. For use in immunoprecipitation and SGK1 kinase assays, full-length and C-terminal fragments of *WNK4* were subcloned into pCDNA3.1 vectors and HA tagged at the amino terminus. All PCR-derived vectors were confirmed by sequencing. Site-directed mutagenesis was used to produce autophosphorylation-deficient full-length *WNK4* (S332A) as well as C-terminal mutants encompassing amino acids 1112–1222. Wild-type *SGK1*, constitutively active *SGK1* (*SGK1/S422D*), and kinase-dead *SGK1* (*SGK1/K127M*) were tagged with FLAG at the amino terminus, and the vector insert was confirmed by sequence analysis.

GST fusion proteins. GST fusion proteins of mouse C-terminal WNK4 for use in SGK1 kinase assays were designed by PCR and site-directed mutagenesis techniques and confirmed by sequencing. GST-WNK4/1112–1222, GST-WNK4/1112–1177, GST-WNK4/1178–1222, GST-WNK4/1127–1179, and corresponding serine-to-alanine mutants, such as S1169A and S1196A, were expressed in BL21 *E. coli* from pGEX 4T1 plasmid (GE Healthcare). GST alone was expressed in BL21 *E. coli* from pGEX 4T3 plasmid (GE Healthcare). GST–L-WNK1 was prepared as previously described (15).

Expression was induced at OD_{600} 0.6 with 1 mM isopropyl-β-D-thiogalactopyranoside and was allowed to proceed for 2 hours at 30°C. Cells were lysed by sonication. GST fusion proteins were purified from sonicates using glutathione sepharose 4B resin (GE Life Science Products) according to the manufacturer's protocol. GST and GST-WNK4 fragments were eluted from the resin with 10 mM glutathione, and the eluted protein was analyzed for quality by SDS-PAGE and Coomassie Blue staining.

Cell culture, transfection, and immunoprecipitation. HEK293 cells transiently transfected with epitope-tagged WNK4 or SGK1 provided lysates to test for coimmunoprecipitation of the index proteins. The cells also supplied lysates with epitope-tagged WNK4 for SGK1 kinase assays.

HEK293 cells were maintained at 37°C, 5% CO_2, in MEM cell culture medium supplemented with 10% fetal bovine serum (Gibco; Invitrogen). Cells were plated on 6-well microtiter plates at a density of 4.25×10^5 cells per well and were transfected the following day with HA-tagged WNK4 pCDNA3.1 (HA-WNK4) constructs. FuGENE 6 transfection reagent (Roche) was used at a ratio of 6 μl FuGENE to 2 μg plasmid, and transfections were carried out in serum-containing growth medium. At 48 hours after transfection, cells were scraped and centrifuged. Collected cells were rinsed 3 times in ice-cold 1× TBS before lysing with ice-cold Lysis/IP buffer (1% Igepal; 150 mM NaCl; 10% glycerol; 20 mM Tris-HCl, pH 8.0; 1 mM EDTA; 0.2% SDS; 2× protease inhibitors set III, Calbiochem; and 2 mM phenylmethanesulphonylfluoride). Lysates were cleared by refrigerated centrifugation, and HA-tagged WNK4 fusion proteins were immunoprecipitated with monoclonal anti-HA agarose (clone HA-7) conjugate (Sigma-Aldrich).

Western blotting and in vitro SGK1 kinase assay. Immunoprecipitated HA-tagged WNK4 constructs were analyzed for protein quality and abundance by Western blotting using monoclonal anti-HA (clone HA-7) antibody (Sigma-Aldrich) and HRP-conjugated anti-mouse IgG secondary antibody (Amersham). HA-tagged mouse WNK4 constructs were eluted from the agarose beads with SDS-PAGE sample buffer prior to gel loading.

Coimmunoprecipitation of WNK4 with SGK1 was determined by testing for the presence of FLAG-tagged SGK1 in Western blot analysis using an anti-FLAG antibody (Sigma-Aldrich) and secondary HRP-conjugated anti-mouse IgG antibody.

HA-tagged WNK4 protein bound to the agarose beads, and GST-WNK4 fusion proteins were tested as substrates for SGK1 using an in vitro kinase assay kit (Upstate Cell Signaling) according to the manufacturer's protocol. Phosphorylation by SGK1 was determined by incorporation of ^{32}P-γ- ATP, visualized by autoradiography, and analyzed by densitometry.

LC/MS/MS. A 50-μl sample of the phosphorylated WNK4 kinase/GST fusion protein — at a 0.1 mg/ml concentration in 20 mM MOPS, pH 7.2; 25 mM β-glycerol phosphate; 5 mM EGTA; and 1 mM orthovanadate buffer — was dried in a vacuum concentrator and dissolved in 10 μl 8M urea, 1.0M Tris (pH 8.5), 8 mM $CaCl_2$, and 0.2M methylamine. Next, 1 μl 0.2M dithiothreitol was added; the sample was incubated at 50°C for 15 minutes; 1 μl 0.5M iodoacetic acid was added; the sample was incubated for an additional 15 minutes at room temperature; the urea concentration was diluted to 2M concentration by addition of water; and 0.2 μg of trypsin was added (Proteomics Grade, product code T6567; Sigma-Aldrich).

After incubation at 37°C overnight, 2 μl of 88% formic acid was added, and 2 μg of digest was analyzed by LC/MS/MS. Peptides were separated using an Agilent 1100 series capillary LC system (Agilent Technologies Inc.) and analyzed using an LTQ linear ion trap mass spectrometer (ThermoFisher). Electrospray ionization was performed with an ion max source fitted with a 34-gauge metal needle (catalog no. 97144-20040; ThermoFisher) and 2.4-kV source voltages. Samples were applied at 20 μl/min to a trap cartridge (Michrom BioResources Inc.), and then switched onto a 0.5 × 250 mm Zorbax SB-C18 column (Agilent Technologies Inc.) using a

mobile phase containing 0.1% formic acid and 7%–30% acetonitrile gradient over 95 minutes at a 10-μl/min flow rate.

Data-dependent collection of MS/MS spectra used the dynamic exclusion feature of the instrument's control software (repeat count, 1; exclusion list size, 50; exclusion duration, 30 seconds; exclusion mass width, –1 to +4) to obtain MS/MS spectra of the 3 most abundant parent ions after each survey scan for the range of m/z 400–2,000. The tune file was configured with no averaging of microscans, a maximum inject time of 200 ms, and AGC targets of 3×10^4 in MS mode and 1×10^4 in Msn mode. Peptides were identified by comparing observed MS/MS spectra with the theoretical fragmentation spectra of peptides generated from a protein database using Sequest (version 27, rev. 12; ThermoFisher). Average parent ion (2.5 tolerance) and average fragment ion (2.0 tolerances) masses were used, along with no enzyme specificity, during the search. A fixed modification of +57 was applied to cysteine residues because of alkylation, and a differential mass of +80 was applied to serine, threonine, and tyrosine residues to search for phosphorylation. We used a *Haemophilus influenzae*–derived decoy database containing 1,775 protein entries supplemented with the sequence of the GST-WNK4 construct. Scaffold (version Scaffold-2-00-05; Proteome Software Inc.) was used to validate MS/MS-based peptide and protein identifications.

Statistics

Xenopus oocyte results were tested for statistically significant differences between conditions by ANOVA with Tukey honestly significantly different test. For LC/MS/MS results used to help identify the location of SGK1 phosphoserine targets at the C-terminal end of WNK4, peptide and protein identifications were accepted when established at greater than 95.0% and 99% probability, respectively.

Acknowledgments

This work was supported by the following grants: NIH KO8 NIDDK 02723, NIH RO1 051496 11, the National Kidney Foundation, and NIH Core Grants 5P30CA069533 and 5P30EY010572.

Received for publication December 15, 2008, and accepted in revised form June 24, 2009.

Address correspondence to: David J. Rozansky, 3181 SW Sam Jackson Park Road, Portland, Oregon 97239, USA. Phone: (503) 494-8081; Fax: (503) 418-6718; E-mail: rozansky@ohsu.edu.

1. Reilly, R.F., and Ellison, D.H. 2000. Mammalian distal tubule: physiology, pathophysiology, and molecular anatomy. *Physiol. Rev.* **80**:277–313.
2. Pearce, D., and Kleyman, T.R. 2007. Salt, sodium channels, and SGK1. *J. Clin. Invest.* **117**:592–595.
3. Verrey, F., Loffing, J., Zecevic, M., Heitzmann, D., and Staub, O. 2003. SGK1: aldosterone-induced relay of Na+ transport regulation in distal kidney nephron cells. *Cell. Physiol. Biochem.* **13**:21–28.
4. Lang, F., et al. 2006. (Patho)physiological significance of the serum- and glucocorticoid-inducible kinase isoforms. *Physiol. Rev.* **86**:1151–1178.
5. von Wowern, F., et al. 2005. Genetic variance of SGK-1 is associated with blood pressure, blood pressure change over time and strength of the insulin-diastolic blood pressure relationship. *Kidney Int.* **68**:2164–2172.
6. Busjahn, A., et al. 2002. Serum- and glucocorticoid-regulated kinase (SGK1) gene and blood pressure. *Hypertension.* **40**:256–260.
7. Flores, S.Y., et al. 2005. Aldosterone-induced serum and glucocorticoid-induced kinase 1 expression is accompanied by Nedd4-2 phosphorylation and increased Na+ transport in cortical collecting duct cells. *J. Am. Soc. Nephrol.* **16**:2279–2287.
8. Velazquez, H., Bartiss, A., Bernstein, P., and Ellison, D.H. 1996. Adrenal steroids stimulate thiazide-sensitive NaCl transport by rat renal distal tubules. *Am. J. Physiol.* **270**:F211–F219.
9. Kim, G.H., et al. 1998. The thiazide-sensitive Na-Cl cotransporter is an aldosterone-induced protein. *Proc. Natl. Acad. Sci. U. S. A.* **95**:14552–14557.
10. Verissimo, F., and Jordan, P. 2001. WNK kinases, a novel protein kinase subfamily in multi-cellular organisms. *Oncogene.* **20**:5562–5569.
11. Wilson, F.H., et al. 2001. Human hypertension caused by mutations in WNK kinases. *Science.* **293**:1107–1112.
12. Wilson, F.H., et al. 2003. Molecular pathogenesis of inherited hypertension with hyperkalemia: the Na-Cl cotransporter is inhibited by wild-type but not mutant WNK4. *Proc. Natl. Acad. Sci. U. S. A.* **100**:680–684.
13. Yang, C.L., Angell, J., Mitchell, R., and Ellison, D.H. 2003. WNK kinases regulate thiazide-sensitive Na-Cl cotransport. *J. Clin. Invest.* **111**:1039–1045.
14. Subramanya, A.R., Yang, C.L., McCormick, J.A., and Ellison, D.H. 2006. WNK kinases regulate sodium chloride and potassium transport by the aldosterone-sensitive distal nephron. *Kidney Int.* **70**:630–634.
15. Yang, C.L., Zhu, X., and Ellison, D.H. 2007. The thiazide-sensitive Na-Cl cotransporter is regulated by a WNK kinase signaling complex. *J. Clin. Invest.* **117**:3403–3411.
16. Kahle, K.T., et al. 2003. WNK4 regulates the balance between renal NaCl reabsorption and K+ secretion. *Nat. Genet.* **35**:372–376.
17. Yang, C.L., Zhu, X., Wang, Z., Subramanya, A.R., and Ellison, D.H. 2005. Mechanisms of WNK1 and WNK4 interaction in the regulation of thiazide-sensitive NaCl cotransport. *J. Clin. Invest.* **115**:1379–1387.
18. Kahle, K.T., Wilson, F.H., and Lifton, R.P. 2005. Regulation of diverse ion transport pathways by WNK4 kinase: a novel molecular switch. *Trends Endocrinol. Metab.* **16**:98–103.
19. Kahle, K.T., Ring, A.M., and Lifton, R.P. 2008. Molecular physiology of the WNK kinases. *Annu. Rev. Physiol.* **70**:329–355.
20. Richardson, C., et al. 2008. Activation of the thiazide-sensitive Na+-Cl- cotransporter by the WNK-regulated kinases SPAK and OSR1. *J. Cell Sci.* **121**:675–684.
21. Chiga, M., et al. 2008. Dietary salt regulates the phosphorylation of OSR1/SPAK kinases and the sodium chloride cotransporter through aldosterone. *Kidney Int.* **74**:1403–1409.
22. Subramanya, A.R., Yang, C.L., Zhu, X., and Ellison, D.H. 2006. Dominant-negative regulation of WNK1 by its kidney-specific kinase-defective isoform. *Am. J. Physiol. Renal Physiol.* **290**:F619–F624.
23. Yang, S.S., et al. 2007. Molecular pathogenesis of pseudohypoaldosteronism type II: generation and analysis of a Wnk4(D561A/+) knockin mouse model. *Cell Metab.* **5**:331–344.
24. Anselmo, A.N., et al. 2006. WNK1 and OSR1 regulate the Na+, K+, 2Cl- cotransporter in HeLa cells. *Proc. Natl. Acad. Sci. U. S. A.* **103**:10883–10888.
25. San-Cristobal, P., et al. 2009. Angiotensin II signaling increases activity of the renal Na-Cl cotransporter through a WNK4-SPAK-dependent pathway. *Proc. Natl. Acad. Sci. U. S. A.* **106**:4384–4389.
26. San-Cristobal, P., Ponce-Coria, J., Vazquez, N., Bobadilla, N.A., and Gamba, G. 2008. WNK3 and WNK4 amino-terminal domain defines their effect on the renal Na+-Cl- cotransporter. *Am. J. Physiol. Renal Physiol.* **295**:F1199–F1206.
27. Lang, F., and Cohen, P. 2001. Regulation and physiological roles of serum- and glucocorticoid-induced protein kinase isoforms. *Sci. STKE.* **2001**:RE17.
28. Bhalla, V., et al. 2005. Serum- and glucocorticoid-regulated kinase 1 regulates ubiquitin ligase neural precursor cell-expressed, developmentally down-regulated protein 4-2 by inducing interaction with 14-3-3. *Mol. Endocrinol.* **19**:3073–3084.
29. Ring, A.M., et al. 2007. An SGK1 site in WNK4 regulates Na+ channel and K+ channel activity and has implications for aldosterone signaling and K+ homeostasis. *Proc. Natl. Acad. Sci. U. S. A.* **104**:4025–4029.
30. Huang, C.L., Cha, S.K., Wang, H.R., Xie, J., and Cobb, M.H. 2007. WNKs: protein kinases with a unique kinase domain. *Exp. Mol. Med.* **39**:565–573.
31. Xu, B., et al. 2000. WNK1, a novel mammalian serine/threonine protein kinase lacking the catalytic lysine in subdomain II. *J. Biol. Chem.* **275**:16795–16801.
32. Min, X., Lee, B.H., Cobb, M.H., and Goldsmith, E.J. 2004. Crystal structure of the kinase domain of WNK1, a kinase that causes a hereditary form of hypertension. *Structure.* **12**:1303–1311.
33. Xu, B.E., et al. 2002. Regulation of WNK1 by an autoinhibitory domain and autophosphorylation. *J. Biol. Chem.* **277**:48456–48462.
34. Ahlstrom, R., and Yu, A.S. 2009. Characterization of the kinase activity of a WNK4 protein complex. *Am. J. Physiol. Renal Physiol.* Online publication ahead of print. doi:10.1152/ajprenal.00358.2009.
35. Masilamani, S., et al. 2002. Time course of renal Na-K-ATPase, NHE3, NKCC2, NCC, and ENaC abundance changes with dietary NaCl restriction. *Am. J. Physiol. Renal Physiol.* **283**:F648–F657.
36. Abdallah, J.G., et al. 2001. Loop diuretic infusion increases thiazide-sensitive Na(+)/Cl(-)-cotransporter abundance: role of aldosterone. *J. Am. Soc. Nephrol.* **12**:1335–1341.
37. O'Reilly, M., et al. 2006. Dietary electrolyte-driven responses in the renal WNK kinase pathway in vivo. *J. Am. Soc. Nephrol.* **17**:2402–2413.
38. Lalioti, M.D., et al. 2006. Wnk4 controls blood pressure and potassium homeostasis via regulation of mass and activity of the distal convoluted tubule. *Nat. Genet.* **38**:1124–1132.
39. Subramanya, A.R. Liu, J. Ellison, D.H. Wade, J.B. and Welling, P.A. 2009. WNK4 diverts the thiazide-sensitive NaCl cotransporter to the lysosome and stimulates AP-3 interaction. *J. Biol. Chem.* In press.
40. Fejes-Toth, G., Frindt, G., Naray-Fejes-Toth, A., and Palmer, L.G. 2008. Epithelial Na+ channel activation and processing in mice lacking SGK1. *Am. J. Physiol. Renal Physiol.* **294**:F1298–F1305.
41. Vallon, V., et al. 2005. SGK1 as a determinant of kidney function and salt intake in response to mineralocorticoid excess. *Am. J. Physiol. Regul. Integr.*

Comp. Physiol. **289**:R395–R401.
42. Hussain, A., et al. 2008. SGK1-dependent upregulation of connective tissue growth factor by angiotensin II. *Kidney Blood Press Res.* **31**:80–86.
43. Murray, J.T., Cummings, L.A., Bloomberg, G.B., and Cohen, P. 2005. Identification of different specificity requirements between SGK1 and PKBalpha. *FEBS Lett.* **579**:991–994.
44. Geraghty, K.M., et al. 2007. Regulation of multisite phosphorylation and 14-3-3 binding of AS160 in response to IGF-1, EGF, PMA and AICAR. *Biochem. J.* **407**:231–241.
45. Huang, C.L., and Kuo, E. 2007. Mechanisms of disease: WNK-ing at the mechanism of salt-sensitive hypertension. *Nat. Clin. Pract. Nephrol.* **3**:623–630.
46. Ring, A.M., et al. 2007. WNK4 regulates activity of the epithelial Na+ channel in vitro and in vivo. *Proc. Natl. Acad. Sci. U. S. A.* **104**:4020–4024.
47. Soundararajan, R., Melters, D., Shih, I.C., Wang, J., and Pearce, D. 2009. Epithelial sodium channel regulated by differential composition of a signaling complex. *Proc. Natl. Acad. Sci. U. S. A.* **106**:7804–7809.
48. Verrey, F., Fakitsas, P., Adam, G., and Staub, O. 2008. Early transcriptional control of ENaC (de)ubiquitylation by aldosterone. *Kidney Int.* **73**:691–696.
49. Wang, W.H., and Giebisch, G. 2009. Regulation of potassium (K) handling in the renal collecting duct. *Pflugers Arch.* **458**:157–168.
50. Chen, S.Y., et al. 1999. Epithelial sodium channel regulated by aldosterone-induced protein sgk. *Proc. Natl. Acad. Sci. U. S. A.* **96**:2514–2519.
51. Wang, J., et al. 2001. SGK integrates insulin and mineralocorticoid regulation of epithelial sodium transport. *Am. J. Physiol. Renal Physiol.* **280**:F303–F313.
52. Zhou, R., and Snyder, P.M. 2005. Nedd4-2 phosphorylation induces serum and glucocorticoid-regulated kinase (SGK) ubiquitination and degradation. *J. Biol. Chem.* **280**:4518–4523.